Title

The microstructure of laminin-111 compensates for dystroglycan loss in mammary epithelial cells in downstream expression of milk proteins.

Authors

Kent, A
Mayer, N
Hochman-Mendez, C
et al.

Publication Date

2019-10-01

DOI

10.1016/j.biomaterials.2019.119337

Peer reviewed

HHS Public Access

Author manuscript

Biomaterials. Author manuscript; available in PMC 2020 July 10.

Published in final edited form as:

Biomaterials. 2019 October ; 218: 119337. doi:10.1016/j.biomaterials.2019.119337.

The microstructure of laminin-111 compensates for dystroglycan loss in mammary epithelial cells in downstream expression of milk proteins

A.J. Kent[a], **N. Mayer**[a], **J.L. Inman**[a], **C. Hochman-Mendez**[b], **M.J. Bissell**[a], **C. Robertson**[a,c,*]

[a]Division of Biological Systems and Engineering, Lawrence Berkeley National Lab, 1 Cyclotron Rd. MS 977, Berkeley, CA, 94720, USA

[b]Regenerative Medicine Research, Texas Heart Institute, Houston TX 77030, USA

[c]Materials Engineering Division, Lawrence Livermore National Lab. 7000 East Ave. Livermore, CA 94550, USA

Abstract

Laminin-111 (Ln-1), an extracellular matrix (ECM) glycoprotein found in the basement membrane of mammary gland epithelia, is essential for lactation. In mammary epithelial cells (MECs), dystroglycan (Dg) is believed to be necessary for polymerization of laminin-111 into networks., thus we asked whether correct polymerization could compensate for Dg loss. Artificially polymerized laminin-111 and the laminin-glycoprotein mix Matrigel, both formed branching, spread networks with fractal dimensions from 1.7 to 1.8, whereas laminin-111 in neutral buffers formed small aggregates without fractal properties (a fractal dimension of 2). In Dg knockout cells, either polymerized laminin-111 or Matrigel readily attached to the cell surface, whereas aggregated laminin-111 did not. In contrast, polymerized and aggregated laminin-111 bound similarly to Dg knock-ins. Both polymerized laminin-111 and Matrigel promoted cell rounding, clustering, formation of tight junctions, and expression of milk proteins, whereas aggregated Ln-1 did not attach to cells or promote functional differentiation. These findings support that the microstructure of Ln-1 networks in the basement membrane regulates mammary epithelial cell function.

Keywords

Laminin; Dystroglycan; Microstructure; Mammary differentiation

*Corresponding author. Materials Engineering Division, Lawrence Livermore National Lab. 7000 East Ave. Livermore, CA, 94550, USA, robertson40@llnl.gov (C. Robertson).

Conflicts of interest

The authors have no conflicts of interest to disclose.

Appendix A. Supplementary data

Supplementary data to this article can be found online at https://doi.org/10.1016/j.biomaterials.2019.119337.

1. Introduction

Laminins in the basement membrane of the mammary gland play a powerful role in regulating the function of epithelial cells [1]. In particular, laminin-111 (Ln-1) is necessary for induction of milk protein expression in mammary epithelial cells (MEC) [2] and induction of proper architecture and quiescence [3,4]. Furthermore, reversion of breast cancer cells to a quiescent phenotype requires appropriate cellLn-1 signaling [5], showing that induction of normal function is intimately coupled with suppression of malignancy [6]. Understanding the mechanisms by which Ln-1 signals to epithelial cells affords new insight into the processes in the breast that regulate normal behavior and suppress malignancy. MECs have a range of receptors for Ln-1 including several integrins, dystroglycan (Dg) and others and these different receptors appear to play different roles in mediating laminin binding and downstream signaling [1,7]. Among the receptors for Ln-1, Dg plays a key role in mediating Ln-1 signaling [8,9] and Dg is frequently lost or alternatively glycosylated in breast and other cancers [10,11].

Dg is known to play multiple roles in laminin signaling: Dg is essential for assembly of laminins in formation of basement membranes [12], Dg links extracellular laminin to cytoskeletal actin [13], and Dg may serve as a nuclear structure factor [14,15]. In mammary epithelia, some evidence suggests that only the basement membrane scaffolding function is necessary, and that linkage to actin or nuclear transcription may at most provide differentiation enhancement. Loss of any of the intracellular domains of Dg does not perturb laminin binding or downstream signaling [8,16], and conversely, loss of the extracellular alpha domain alone perturbs the cells ability to bind and respond to laminin [8,17]. Furthermore, the extracellular domains of Dg grafted onto the transmembrane domain of a different protein is sufficient for Ln-1 binding to the cell surface and induction of milk proteins [8]. This suggests that Dg in the mammary gland does not directly transduce Ln-1 and instead acts through other mechanisms. However, the complex laminin-rich mixture of proteins secreted by Engelbreth-Holm-Swarm tumors (sold commercially as Matrigel) does not show this same dependence on Dg for laminin anchorage [8], and deletion of Dg in the mammary gland does not appear to impair basement membrane formation in vivo [16]. Thus, the mechanism by which Dg acts in laminin signaling in MEC remains unclear.

We directly tested the hypothesis that Dg is necessary for MEC function because it polymerizes laminin into a basement membrane-like layer in the mammary gland. We used a method to artificially generate a hexagonal lattice of laminin proteins resembling the innermost layer of the basement membrane [18]. We then compared these networks structurally to the laminin networks in Matrigel, tested whether Dg knockout and knock in cells were sensitive to microstructural changes in purified laminin, and evaluated whether synthesis of milk proteins and cell morphology changes could be induced by correctly structured laminin.

2. Materials and methods

2.1. Laminin polymerization

Purified laminin-111 from Engelbreth-Holm-Swarm/Matrigel was purchased from Invitrogen (23017015). Growth factor reduced Matrigel was purchased from Corning (356230). Laminin-11 was then polymerized into polyLM or pH7-Ln as described in Ref. [18]. Briefly, polyLM was created by mixing 100 μg/mL Ln-1 with 1 mM $CaCl_2$ and 20 mM sodium acetate at pH4, which was then incubated for 30 min at 37 °C, and then spun down at 2000 rcf. pH7-Ln was created by mixing 100 μg/mL Ln-1 with 1 mM $CaCl_2$ and 20 mM Tris at pH7, which was then incubated for 30 min at 37 °C then spun down at 20,000 rcf. The pellets were then resuspended in cell culture media for adsorption to glass slides or for addition to cells in culture. For laminin-nidogen-1 copolymers, we mixed laminin at 50 μg/mL with 50 μg/mL recombinant nidogen-1 (R&D systems 2570-Nd-050), then spun down at 2,000rcf and resuspended in cell culture media.

For fluorescently labeled laminin experiments, HiLight488 labeled laminin-111 (LMN02, Cytoskeleton Inc) was added to unlabeled laminin at a ratio of 1:50, then treated according to either polyLM or pH7 protocols as described previously.

2.2. Cell culture

Murine mammary MEC were cultured as previously described [8]. Briefly, Dg knockout cells and a subline with Dg restored by knock-in were seeded at 8 K cells/cm^2 for DgKO or 5 K cells/cm^2 for DgKI to account for differences in growth rate and cultured in DMEM-F12 (Gibco 11330) supplemented with 2% FBS, 0.01 mg/mL Insulin (Sigma-Aldrich I-1882), 0.005 μg/mL EGF (BD Bioscience 354001), 0.05 mg/ mL Gentamicin (Thermo-Fisher 15750060), and 0.05 mg/mL Normocin (InvivoGen ant-nr-1) in 37 °C, humidified incubators at 5% CO_2 tension. Cells were passed every 4–5 days by treatment with 0.25% trypsinEDTA, neutralized with cell culture media, spun down at 115 rcf for 5 min, and resuspended in media.

For laminin overlay procedures, cells were seeded at 10.5 K cells/ cm^2 and grown for 2 days, then treated with Matrigel (Mg-Ln), polyLM or pH7-Ln in induction media comprised of DMEM-F12 supplemented with 3 μg/mL prolactin (National Hormone and Peptide Program, Ovine PRL 10 mg), 2.8 μM hydrocortisone (Sigma-Aldrich H-0888 1G), and 5 μg/mL insulin (Sigma-Aldrich I-1882). Cells were then cultured for 2 days before collection for analysis by immunostaining or Western blot as described below.

2.3. Immunostaining

Ln-1 polymers and cell cultures were fixed with 4% paraformaldehyde in PBS, blocked with 10% goat serum plus Fab fragment (Jackson ImmunoResearch 715–007-003) to block endogenous mouse antibodies, then stained with an anti-laminin antibody (Sigma L9393) or anti-ZO-1 (Invitrogen 61–7300) overnight at 4 °C, followed by Alexafluor conjugated secondary antibodies (Invitrogen A-11034) and DAPI (4′,6-Diamidino-2-Phenylindole, Dihydrochloride, Invitrogen D1306). Alexafluor labeled phalloidins (Invitrogen A12379) was used according to manufacturer's instructions for staining filamentous actin.

2.4. Microscopy and image analysis

Widefield microscopy was performed on an upright Zeiss Axioimager and confocal microscopy was performed on a Zeiss LSM 710 scope with a 63X/1.4NA objective. Pinhole was set to one Airy unit. Images of laminin networks were processed to measure the box counting dimension in MATLAB (Mathworks, Natick). Cross correlation and autocorrelation functions were calculated using Fourier transforms, then fit with a 2-Dimensional Gaussian functions in MATLAB as described previously [19–21].

2.5. Scanning electron microscopy

Mg-Ln, polyLM and pH7-Ln were treated as described above, spun down and resuspended in cell culture media (pH7.4) and allowed to adsorb onto silica wafers for 90 min. Laminin matrices were fixed in 2.5% glutaraldehyde in 0.1 M sodium cacodylate buffer at pH7.4, washed three times with 0.1 M sodium cacodylate buffer at pH7.2, postfixed 1 h in 1% osmium tetroxide in 0.1 M sodium cacodylate buffer at pH7.2, washed three times in 0.1 M sodium cacodylate buffer at pH7.2, then dehydrated through increasing concentrations of ethanol and sputter coated with a thin layer of gold. Samples were imaged on a Hitachi S-5000 scanning electron microscope.

2.6. Western blotting

For western blotting, cells were harvested in RIPA buffer with protease inhibitor cocktail set 1 (Calbiochem 539,131–10VL) and phosphatase inhibitor sets 1 and 2 (Sigma-Aldrich P2850–5 ML and P5726–5 ML, respectively) on ice and then sheared through a 29G insulin needle and then spun down for 20 min at 21,000 rcf. Supernatants were then transferred to fresh tubes and the protein concentration was determined using a Lowry Assay (DC Protein Assay Bio Rad 500–0115). Protein samples were loaded on 4–20% Tris-Gly gradient gels (Invitrogen XP04200BOX), electrophoresed, and then transferred to nitrocellulose membranes with a dry transfer system (Invitrogen iBlot Blotting System and Gel Transfer Stacks Invitrogen IB301001). Membranes were stained with anti-laminin (Sigma L9393), rabbit polyclonal anti-β casein (developed by Caroline Kaetzel [22]), antilamin B1 (Abcam ab16048) or anti-α-tubulin (Santa Cruz 32293).

2.7. Statistical analyses

ANOVA analyses and Tukey’s posthoc tests were performed in MATLAB with a significance level of $p < 0.05$.

3. Results

3.1. PolyLM laminin networks are structurally similar to laminin-glycoprotein mixes

To determine why Dg is necessary for Ln-1 signaling in epithelial cells, we cultured MECs in the presence of the lactogenic hormones and an overlay of purified Ln-1. Specifically we compared mouse MEC from a conditional Dg knockout (DgKO) to cells from this line with Dg expression was restored by knock-in (DgKI) (created in Ref. [8], Dg expression confirmed in Supplemental Fig. 1). We observed that Ln-1 on the surface of DgKI cells formed web-like networks, whereas in acellular regions Ln-1 formed small aggregates (Fig.

1A and insert). In DgKO cultures, similar aggregates were observed in acellular regions, but minimal Ln-1 was observed on the surface of cells (Fig. 1B and insert).

We compared the microstructure of acellular purified Ln-1 aggregated in neutral buffered solutions (pH7-Ln), to the Ln-1 network formed in the laminin-glycoprotein mix Matrigel (Mg-Ln), to polymerized purified Ln-1 (polyLM) [23–25]. Neutral buffer-treated laminin adsorbed to glass in neutral buffered media formed small aggregates (Fig. 1C), whereas Mg-Ln and polyLM formed branched, space filling polymers (Fig. 1D&E). To evaluate why Mg-Ln in neutral buffered media showed such a different network structure than purified Ln-1 in the same conditions, we mixed Ln-1 with recombinant nidogen-1 (Nd1-Ln) and observed network formation similar to Mg-Ln and polyLM (Fig. 1F). Interestingly, switching from phosphate buffered saline to tris buffered saline destroyed the network structure of Ln for each of these conditions, suggesting that pH control may underlie network assembly (Supplemental Fig. 2).

As previous work has demonstrated that polymerized laminin has fractal properties [23], we quantitatively compared network morphology, using the both box counting algorithm and power spectrum analysis to estimate the fractal dimension of these images. We found that Mg-Ln, polyLM, and Nd1-Ln had fractal dimensions of approximately 1.7, consistent with previous work [23] (Fig. 1G), whereas pH7-Ln had a dimension of approximately 2, indicating no fractal properties. Power spectrum analysis, an alternative method to measure the microstructure of fractal images without thresholding [20], likewise showed similar properties for Mg-Ln, polyLM, and Nd1-Ln and dramatically different measures for pH7-Ln (Fig. 1H). Thus, the Ln-1 networks formed in Mg-Ln, polyLM, and Nd1-Ln were structurally similar, whereas pH7-Ln had markedly different morphological properties.

To confirm these findings using higher resolution imaging, we collected pH7-Ln, polyLM, and Mg-Ln onto silica wafers, then processed these samples for scanning electron microscopy (Fig. 2A–F). We observed a lacy network structure in polyLM and Mg-Ln which was absent in pH7-Ln conditions suggesting that Mg-Ln and polyLM show similar organized network structure (Fig. 2D).

3.2. The microstructure of laminin alters its binding to DgKO but not to DgKI cells

Next, we compared whether equivalent amounts of polyLM and pH7-Ln could bind to cells with and without Dg. We performed Lowry assays and western blots to confirm equivalent quantities of Ln-1 were used for stimulus (Supplemental Fig. 3). PolyLM and pH7-Ln adhered to the surface of DgKI cells by immunofluorescence (Fig. 3Ai and ii) and Western blot (Fig. 3C). No difference in polyLM and pH7-Ln bound to DgKI cells was detected by Western blot or immunofluorescence ($p > 0.5$) (Fig. 3Ei and ii). In DgKO cells, polyLM adhered to cells readily (Fig. 3Bi and D) whereas pH7-Ln failed to bind (Fig 3 bii and 3D) and the amount of Ln-1 bound to cells in polyLM was significantly higher than in pH7-Ln conditions by both Western blot and immunofluorescence (Fig 3Fi and ii).

We next investigated whether Ln-1 levels derived from anchorage of exogenously provided laminin or from endogenous Ln-1 production. The laminin antibody used in this work detects both stimulus laminin and endogenous production (Supplemental Fig. 3A). We

repeated these experiments using fluorescently labeled Ln-1 to mark the exogenous stimulus, then immunostained for laminin to measure both endogenous and exogenous laminin (Fig. 4 A and B). We then calculated the intensity of the labeled laminin and the total laminin for each pixel in these images and plotted the frequency distribution of both intensities in a 2D histogram (Fig. 4C and D). In DgKO cells stimulated with pH7-Ln (Fig. 4C), we observed that most pixels with high antibody staining were dark in the labeled laminin channel, thus these pixels likely represent endogenous laminin production. In DgKO cells stimulated with polyLM (Fig. 4D), we observed two populations of pixel intensities on the 2D histogram, one bright in the antibody channel and dark in the labeled laminin channel, which represents endogenous production, and one bright in both channels, which represents the exogenous stimulus of labeled laminin.

To quantitatively compare endogenous production and stimulus across images, we then measured the total number of pixels with antibody intensity of >20 and labeled laminin intensity of <20, and intensity of >20 for both channels (Fig. 4E). Notably, the endogenous production is present in both conditions but appears to be greater in the polyLM condition than in the pH7-Ln condition. This shows that engagement of Ln-1 with the surface of cells requires either Dg or glycoproteins or correctly polymerized Ln-1.

3.3. PolyLM induces functional differentiation of Dg knockout MEC

Given that polymerizing Ln-1 restored its adhesion to cells, we next asked in DgKO MEC if Ln-1 microstructure could induce differentiation by four standard metrics of MEC function: induction of β-casein expression, colony morphology, tight junction formation, and reduction of cytoplasmic actin and actin stress fibers.

First, we compared expression of the milk protein β-casein across polyLM and pH7-Ln conditions. We observed significantly higher expression of β-casein in polyLM conditions compared to pH7-Ln (Fig. 5A and B). This confirmed that the difference in Ln-1 binding between polyLM and pH7-Ln translates to functional differences.

We then compared functional differentiation using increasing doses of Mg-Ln, polyLM and pH7-Ln (Fig. 5C–H), and observed increased laminin staining, increased β-casein staining and a colony morphology shift. Quantitative image analysis revealed increasing laminin and β-casein in both the Mg-Ln and polyLM (Fig. 5I and J) conditions but not in pH7-Ln conditions (pH7-Ln at 800 μg/ml was not different from pH7-Ln at 100 μg/ml). Notably, polyLM at 800 μg/mL and Mg-Ln at 50 μg/ mL were not statistically different with respect to Ln-1 anchorage or β-casein expression.

Concomitant with induction of β-casein expression, we observed a colony morphology change from the relatively flat, spread colonies (Fig. 5C and D) to the formation of tubular colonies with increasing doses of both Mg-Ln and polyLM (Fig. 5F and G and Supplemental Fig. 4). These morphological changes were not observed even at the highest tested dose (800 μg/ml) of pH7-Ln (Fig. 5I). To quantify these changes in cell colony morphology, we calculated the autocorrelation of the images of nuclei, which measures the likelihood that 2 pixels separated by a given vector in an image are both bright, then used Gaussian fitting to estimate the falloff of this probability [19,20] (Fig. 5K). Comparing across Ln treatment and

concentration, we observed that cells in Mg-Ln at 50 or 100 μg/ml or polyLM at 800 μg/ml showed statistically higher aggregation compared to pH7-Ln at 800 μg/ ml by two-way ANOVA and Tukey's post hoc test (Fig. 5K).

Given this formation of tubular cell colonies, we next investigated cell junction and cytoskeletal organization. In Mg-Ln or polyLM, the majority of actin in the cell body colocalized with ZO-1 in the cell-cell junctions and almost no stress fiber formation was observed (Fig. 6A and B). In pH7-Ln and control conditions, MEC formed abundant stress fibers at the basal surface (Fig. 6 C and D, indicated by white arrows). To quantify these changes, we first measured the ratio of filamentous actin stained with phalloidin to nuclei stained with DAPI, and we observed a higher ratio in either pH7-Ln or control conditions relative to polyLM or Mg-Ln (Fig. 6E), indicating greater stress fiber abundance.

In both the polyLM and Mg-Ln conditions, we observed continuous apical tight junctions containing both zonula occludens-1 (ZO-1) and filamentous actin (Fig. 6A and B), whereas interrupted ZO-1 staining was observed in either pH7-Ln or control no-Ln-1 conditions (Fig. 6C and D, indicated by gray arrows). We calculated the cross correlation of ZO-1 and actin, which measures the probability that bright pixels in ZO-1 channel are near bright pixels in the actin channel and vice versa. One-way ANOVA on the cross correlation demonstrated that ZO-1 and actin were more likely to be colocalized in Mg-Ln or polyLM than in either pH7-Ln or cells treated with hormones but no laminin (control) (Fig. 6F), and association of ZO-1 and actin in pH7-Ln and control conditions was not statistically different. Thus, while more actin was observed in pH7-Ln and control conditions, actin in Mg-Ln and polyLM conditions were more likely to be found at cell-cell junctions.

Given this decrease of actin and increase of actin in cell-cell junctions we checked whether cortical actin tended to be linked to laminin in Mg-Ln and polyLM conditions. We determined that cortical actin and laminin were anticorrelated in both Mg-Ln and polyLM conditions in DgKI cells (Supplemental Fig. 5) and DgKO cells (not shown). Next, we investigated the receptor for Ln-1 in DgKO cells, using function blocking antibodies. We found that binding of both Mg-Ln and polyLM to DgKO cells was abrogated in the presence of integrin β1 function blocking antibodies.

4. Discussion

In this work, we demonstrated that MEC function depends on Ln-1 microstructure and that this change in anchorage regulates milk protein expression and cell shape. We found that multiple mechanisms give rise to similar Ln-1 microstructures. Ln-1 polymerized into a fractal network in the presence of Dg, acidic proteoglycans such as those found in Matrigel, or acidic buffered calcium solutions, suggesting these mechanisms can compensate for each other. We found that polymerized Ln-1 formed a coherent coat on the cell surface and induced cell shape changes and β-casein expression. The complex mixture of laminins and glycoproteins in Mg-Ln was more efficient in inducing these changes than polyLM.

That Dg is dispensable for induction of β-casein is surprising. In myocytes, Dg is necessary to sarcomere anchorage and organization and thus prevents a form of muscular dystrophy

[26,27]. In contrast we found that cortical actin and Ln-1 were anti-correlated in MEC, with less cortical actin in regions where Ln-1 bound to the cell surface, demonstrating tissue specific differences in how Ln-1 is sensed (Supplemental Fig. 6). Nonetheless, the frequent loss or aberrant sum of intensity of DAPI staining. glycosylation of Dg in breast cancers suggests that it plays an important role in healthy breast epithelia [8].

Similar microstructures were created by both cell surface Dg and basement membrane proteoglycans, suggesting compensation between these mechanisms for polymerizing Ln-1 in some cases. Indeed, both Dg and Nidogen-1 knockout mice show essentially normal basement membrane formation and maintenance in epithelial tissues [28–31], suggesting that the compensation we observed in vitro may occur in vivo. We have demonstrated that polymerized Ln-1 can compensate for Dg loss, raising the question of how Ln-1 microstructure alters avidity of Ln-1 for cells.

Ln-1 is a trimeric, cross-shaped protein with different adhesive domains on the ends of the three short arms and one long arm: thus the polymerization state may relate to the cell display of these different domains [32]. A number of laminin receptors bind only to the globular domains on the long arm or only to the short arms [33,34]. At neutral pH in the presence of calcium, Ln-1 forms small aggregates which we believe results from mixed short arm-short arm and short arm-long arm binding [23]. In contrast, lowering the pH appears to preferentially charge the long arm globular domains of Ln-1, resulting in electrostatic repulsion between long arms and increased probability of short arm-short arm binding [23]. As a result, polymerization in acidic conditions appears to increase long arm display.

Previous work suggests that nidogen-1 (Nd-1) and other glycoproteins crosslink specific domains on the long arm of Ln-1 [24]. It is therefore surprising that Mg-Ln or Nd1-Ln polymerized similarly to polyLM. As reported previously [35], we found that Ln-1 polymerized into a self-similar network with fractal dimension of ~1.7, characteristic of diffusion limited aggregation. Indeed, previous work shows that polyLM polymerization follows a nucleation and growth schema [23] which defines diffusion limited aggregation phenomena. This suggests that laminin-glycoprotein mixes undergo similar aggregation processes for assembly. We found that buffer systems with higher buffering capacity reduced the ability of nidogen-1 and other glycoproteins to promote polymerization. This suggests that the electrostatic effects of negatively charged glycoproteins on Ln-1 may be important (Supplemental Fig. 2).

In all culture conditions tested, Mg-Ln was more efficient than polyLM alone in binding to MEC and inducing functional differentiation, suggesting that the additional protein components in Mg-Ln play some role in cell signaling and/or Ln-1 organization. Here we found that at similar total protein concentrations Mg-Ln formed coherent Ln-1 coats whereas polyLM formed patches. This finding is supported by previous work showing that while Nd-1 by itself does not induce β-casein expression in mammary cells, Nd1-Ln mixes are more effective than Ln-1 alone [36,37].

We postulate that this enhancement is due to reinforcement of Ln-1 networks by other proteins or glycoproteins. Previous work has demonstrated that while Ln-1 is sufficient for

initial formation of basement membranes, reinforcement with other proteins such as collagen IV is required for basement membrane stability [38]. Formation of apical polarity in epithelial cells has been previously, linked previously to collagen IV reinforcement [39]. In agreement, we observed occasional formation of lumens in Mg-Ln conditions but not in polyLM. This demonstrates that while polymerized Ln-1 is sufficient for induction of β-casein, it may not be sufficient for induction of all mammary epithelial specific phenotypes.

5. Conclusions

In summary, we conclude that microstructure of Ln-1 networks in the basement membrane regulates epithelial cell function. We found that polymerized Ln-1 could come from either cell surface Dg or basement membrane glycoproteins. In DgKO cells, polymerized Ln-1 can alter cell morphology, tight junction assembly, and milk protein expression.

Supplementary Material

Refer to Web version on PubMed Central for supplementary material.

Acknowledgements

This work funded by the DOD CDMRP Breast Cancer Research Program BC133875, the L'Oreal USA for Women in Science Program, and Lawrence Livermore National Lab LDRD 18-ERD-062 (to C.R.), NIH R01CA064786, DOD Breast Cancer Research Program and the Breast Cancer Research Foundation (to MJB). Thanks to John Muschler for his kind gift of the DgKO and DgKI cells. Thank you to the staff at the University of California Berkeley Electron Microscope Laboratory for advice and assistance in electron microscopy sample preparation and data collection. Thanks to Cerise Bennett, Gita Rohanitazangi, Simone Skiba, Kate Thi, and Josephine Wu for their help with the work and to Monica Moya for her helpful comments on this work and to Jonathan Adorno and Olivia McIntosh for their help with editing.

This work was performed under the auspices of the U.S. Department of Energy by Lawrence Livermore National Laboratory under Contract DE-AC52-07NA27344. IM release: LLNL-JRNL-766544

The raw data required to reproduce these findings are available from the corresponding author.

References

[1]. Yurchenco PD, Integrating activities of laminins that drive basement membrane assembly and function, Curr. Top. Membr 76 (2015) 1–30. [PubMed: 26610910]

[2]. Li ML, Aggeler J, Farson DA, Hatier C, Hassell J, Bissell MJ, Influence of a reconstituted basement membrane and its components on casein gene expression and secretion in mouse mammary epithelial cells, Proc. Natl. Acad. Sci. U. S. A 84 (1) (1987) 136–140. [PubMed: 3467345]

[3]. Spencer VA, Costes S, Inman JL, Xu R, Chen J, Hendzel MJ, Bissell MJ, Depletion of nuclear actin is a key mediator of quiescence in epithelial cells, J. Cell Sci 124 (1) (2011) 123–132. [PubMed: 21172822]

[4]. Fiore APZP, Spencer VA, Mori H, Carvalho HF, Bissell MJ, Bruni-Cardoso A, Laminin-111 and the level of nuclear actin regulate epithelial quiescence via exportin-6, Cell Rep. 19 (10) (2017) 2102–2115. [PubMed: 28591581]

[5]. Weaver VM, Petersen OW, Wang F, Larabell CA, Briand P, Damsky C, Bissell MJ, Reversion of the malignant phenotype of human breast cells in three-dimensional culture and in vivo by integrin blocking antibodies, J. Cell Biol 137 (1) (1997) 231–245. [PubMed: 9105051]

[6]. Bissell MJ, Hines WC, Why don't we get more cancer? A proposed role of the microenvironment in restraining cancer progression, Nat. Med 17 (3) (2011) 320–329. [PubMed: 21383745]

[7]. Muschler J, Lochter A, Roskelley CD, Yurchenco P, Bissell MJ, Division of labor among the alpha6beta4 integrin, beta 1 integrins, and an E3 laminin receptor to signal morphogenesis and beta-casein expression in mammary epithelial cells, Mol. Biol. Cell 10 (1999).

[8]. Weir ML, Oppizzi ML, Henry MD, Onishi A, Campbell KP, Bissell MJ, Muschler JL, Dystroglycan loss disrupts polarity and β-casein induction in mammary epithelial cells by perturbing laminin anchoring, J. Cell Sci 119 (19) (2006) 4047–4058. [PubMed: 16968749]

[9]. Muschler J, Lochter A, Roskelley CD, Yurchenco P, Bissell MJ, Division of labor among the α6β4 integrin, β1 integrins, and an E3 laminin receptor to signal morphogenesis and β-casein expression in mammary epithelial cells, Mol. Biol. Cell 10 (9) (1999) 2817–2828. [PubMed: 10473629]

[10]. Weir ML, Muschler J, Dystroglycan: emerging roles in mammary gland function, J. Mammary Gland Biol. Neoplasia 8 (4) (2003) 409–419. [PubMed: 14985637]

[11]. Henry MD, Cohen MB, Campbell KP, Reduced expression of dystroglycan in breast and prostate cancer, Hum. Pathol 32 (8) (2001) 791–795. [PubMed: 11521221]

[12]. Williamson RA, Henry MD, Daniels KJ, Hrstka RF, Lee JC, Sunada Y, Ibraghimov-Beskrovnaya O, Campbell KP, Dystroglycan is essential for early embryonic development: disruption of Reichert's membrane in Dag1-null mice, Hum. Mol. Genet 6 (6) (1997) 831–841. [PubMed: 9175728]

[13]. Colognato H, Winkelmann DA, Yurchenco PD, Laminin polymerization induces a receptor–cytoskeleton network, J. Cell Biol 145 (3) (1999) 619–631. [PubMed: 10225961]

[14]. Mathew G, Mitchell A, Down JM, Jacobs LA, Hamdy FC, Eaton C, Rosario DJ, Cross SS, Winder SJ, Nuclear targeting of dystroglycan promotes the expression of androgen regulated transcription factors in prostate cancer, Sci. Rep 3 (2013) 2792. [PubMed: 24077328]

[15]. Martínez-Vieyra IA, Vásquez-Limeta A, González-Ramírez R, Morales-Lázaro SL, Mondragón M, Mondragón R, Ortega A, Winder SJ, Cisneros B, A role for β-dystroglycan in the organization and structure of the nucleus in myoblasts, Biochim. Biophys. Acta Mol. Cell Res 1833 (3) (2013) 698–711.

[16]. Leonoudakis D, Singh M, Mohajer R, Mohajer P, Fata JE, Campbell KP, Muschler JL, Dystroglycan controls signaling of multiple hormones through modulation of STAT5 activity, J. Cell Sci. 123 (21) (2010) 3683–3692. [PubMed: 20940259]

[17]. Muschler J, Levy D, Boudreau R, Henry M, Campbell K, Bissell MJ, A role for dystroglycan in epithelial polarization: loss of function in breast tumor cells, Cancer Res. 62 (23) (2002) 7102–7109. [PubMed: 12460932]

[18]. Freire E, Coelho-Sampaio T, Self-assembly of laminin induced by acidic pH, J. Biol. Chem 275 (2) (2000) 817–822. [PubMed: 10625612]

[19]. Merna N, Robertson C, La A, George SC, Optical imaging predicts mechanical properties during decellularization of cardiac tissue, Tissue engineering, Part C, Methods 19 (10) (2013) 802–809. [PubMed: 23469868]

[20]. Robertson C, George SC, Theory and practical recommendations for autocorrelation-based image correlation spectroscopy, J. Biomed. Opt 17 (8) (2012) 080801–1. [PubMed: 23224160]

[21]. Robertson C, Ikemura K, Krasieva TB, George SC, Multiscale analysis of collagen microstructure with generalized image correlation spectroscopy and the detection of tissue prestress, Biomaterials 34 (26) (2013) 6127–6132. [PubMed: 23642533]

[22]. Lee EY, Lee WH, Kaetzel CS, Parry G, Bissell MJ, Interaction of mouse mammary epithelial cells with collagen substrata: regulation of casein gene expression and secretion, Proc. Natl. Acad. Sci. U. S. A 82 (5) (1985) 1419–1423. [PubMed: 3856271]

[23]. Hochman-Mendez C, Cantini M, Moratal D, Salmeron-Sanchez M, Coelho-Sampaio T, A fractal nature for polymerized laminin, PLoS One 9 (10) (2014) e109388. [PubMed: 25296244]

[24]. Yurchenco PD, Cheng YS, Schittny JC, Heparin modulation of laminin polymerization, J. Biol. Chem 265 (7) (1990) 3981–3991. [PubMed: 2303489]

[25]. Yurchenco PD, Smirnov S, Mathus T, Analysis of basement membrane self-assembly and cellular interactions with native and recombinant glycoproteins, Methods Cell Biol. 69 (2002) 111–144. [PubMed: 12070988]

[26]. Cote PD, Moukhles H, Lindenbaum M, Carbonetto S, Chimaeric mice deficient in dystroglycans develop muscular dystrophy and have disrupted myoneural synapses, Nat. Genet 23 (3) (1999) 338–342. [PubMed: 10610181]

[27]. Chen Y-J, Spence HJ, Cameron JM, Jess T, Ilsley JL, Winder SJ, Direct interaction of beta-dystroglycan with F-actin, Biochem. J 375 (Pt 2) (2003) 329–337. [PubMed: 12892561]

[28]. Murshed M, Smyth N, Miosge N, Karolat J, Krieg T, Paulsson M, Nischt R, The absence of nidogen 1 does not affect murine basement membrane formation, Mol. Cell. Biol 20 (18) (2000) 7007–7012. [PubMed: 10958695]

[29]. Esser AK, Cohen MB, Henry MD, Dystroglycan is not required for maintenance of the luminal epithelial basement membrane or cell polarity in the mouse prostate, Prostate 70 (7) (2010) 777–787. [PubMed: 20054819]

[30]. Jarad G, Pippin JW, Shankland SJ, Kreidberg JA, Miner JH, Dystroglycan does not contribute significantly to kidney development or function, in health or after injury, Am. J. Physiol. Renal. Physiol 300 (3) (2011) F811–F820. [PubMed: 21209007]

[31]. Bader BL, Smyth N, Nedbal S, Miosge N, Baranowsky A, Mokkapati S, Murshed M, Nischt R, Compound genetic ablation of nidogen 1 and 2 causes basement membrane defects and perinatal lethality in mice, Mol. Cell. Biol 25 (15) (2005) 6846–6856. [PubMed: 16024816]

[32]. Colognato H, Yurchenco PD, Form and function: the laminin family of heterotrimers, Dev. Dynam 218 (2) (2000) 213–234.

[33]. Kortesmaa J, Yurchenco P, Tryggvason K, Recombinant laminin-8 (alpha(4)beta(1)gamma(1)). Production, purification,and interactions with integrins, J. Biol. Chem 275 (20) (2000) 14853–14859. [PubMed: 10809728]

[34]. Nishiuchi R, Takagi J, Hayashi M, Ido H, Yagi Y, Sanzen N, Tsuji T, Yamada M, Sekiguchi K, Ligand-binding specificities of laminin-binding integrins: a comprehensive survey of laminin–integrin interactions using recombinant α3β1, α6β1, α7β1 and α6β4 integrins, Matrix Biol. 25 (3) (2006) 189–197. [PubMed: 16413178]

[35]. Daccord G, Nittmann J, Stanley HE, Radial viscous fingers and diffusion-limited aggregation: fractal dimension and growth sites, Phys. Rev. Lett 56 (4) (1986) 336–339. [PubMed: 10033161]

[36]. Streuli CH, Schmidhauser C, Bailey N, Yurchenco P, Skubitz AP, Roskelley C, Bissell MJ, Laminin mediates tissue-specific gene expression in mammary epithelia, J. Cell Biol 129 (3) (1995) 591–603. [PubMed: 7730398]

[37]. Pujuguet P, Simian M, Liaw J, Timpl R, Werb Z, Bissell MJ, Nidogen-1 regulates laminin-1-dependent mammary-specific gene expression, J. Cell Sci 113 (5) (2000) 849–858. [PubMed: 10671374]

[38]. Pöschl E, Schlötzer-Schrehardt U, Brachvogel B, Saito K, Ninomiya Y, Mayer U, Collagen IV is essential for basement membrane stability but dispensable for initiation of its assembly during early development, Development 131 (7) (2004) 1619–1628. [PubMed: 14998921]

[39]. Plachot C, Chaboub LS, Adissu HA, Wang L, Urazaev A, Sturgis J, Asem EK, Lelièvre SA, Factors necessary to produce basoapical polarity in human glandular epithelium formed in conventional and high-throughput three-dimensional culture: example of the breast epithelium, BMC Biol. 7 (2009) 77–77. [PubMed: 19917093]

HIGHLIGHTS

- Laminin assembles into a fractal network in presence of either the receptor dystroglycan or acidic glycoproteins or an acidic buffer.
- When this microstructure is recreated with acidic treatment, laminin binds readily to dystroglycan null cells.
- Microstructured laminin induces dystroglycan null mammary epithelial cells to functionally differentiate to milk producing cells.

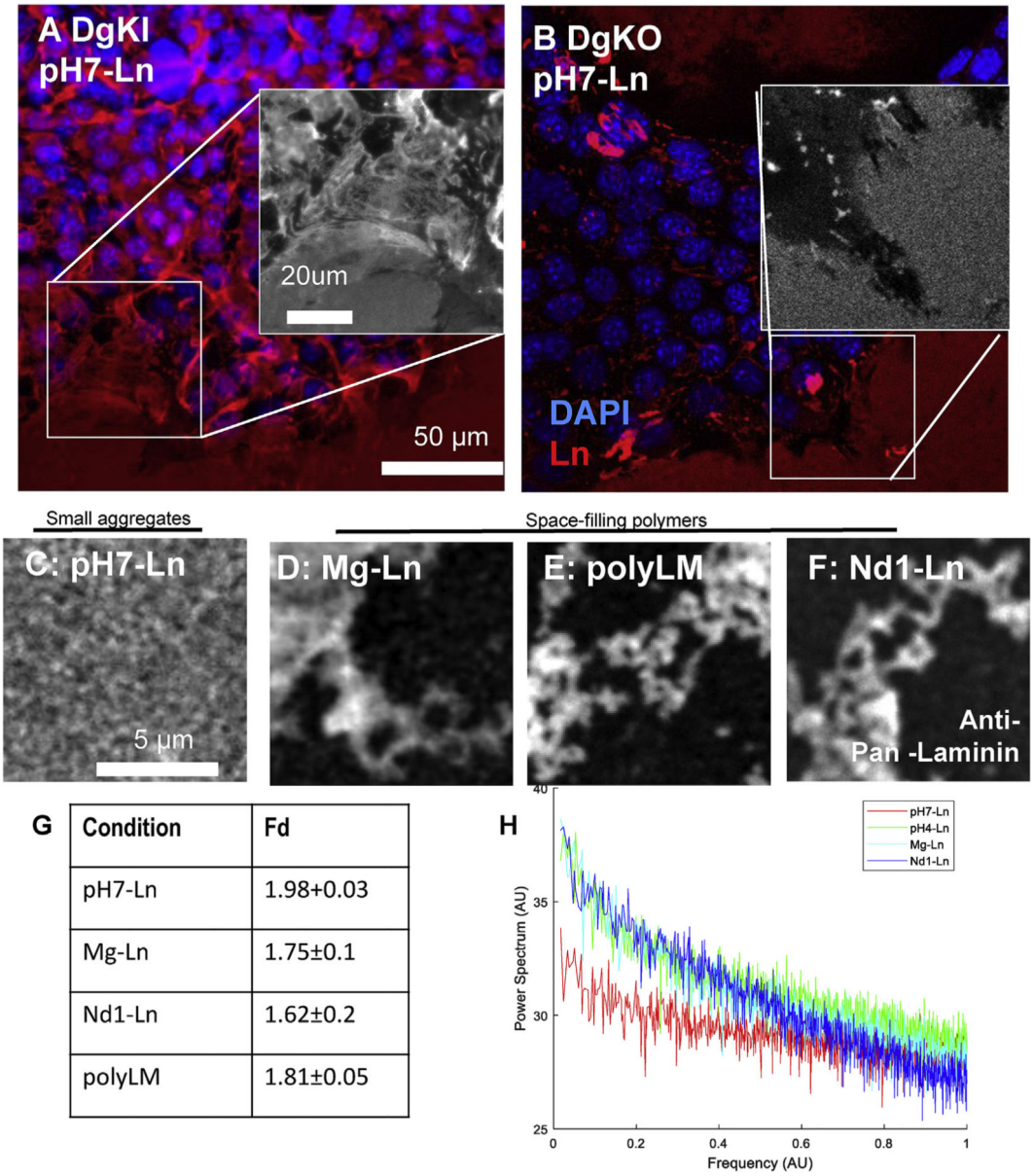

Condition	Fd
pH7-Ln	1.98+0.03
Mg-Ln	1.75±0.1
Nd1-Ln	1.62±0.2
polyLM	1.81±0.05

Fig. 1.

Fractal laminin polymerization occurs naturally on DgKI cells and artificially in acidic conditions. A. Immunofluorescence of purified Ln-1 on DgKI cells at pH7 shows that laminin adheres and forms a lacy network. Inset: laminin network on the cell surface shows a different morphology compared to on the glass, B. Immunofluorescence of purified Ln-1 on DgKO at pH7 shows that laminin fails to adhere to Dg null cells. Inset: almost no laminin is observed on the cell surface and laminin adhered to glass in acellular regions forms globules. C. Laminin in a neutral pH7 buffer forms small, round agglomerations. D. Laminin network in the laminin-glycoprotein mix Matrigel ™ (Mg-Ln) forms web-like networks. E. Laminin in an acidic pH4 buffer (polyLM) forms a web-like network similar to that of Mg-Ln. F. Laminin in the presence of the acidic glycoprotein Nidogen (Nd1-Ln) forms a polymerized laminin network similar to that of Mg-Ln. G. Fractal dimensions calculated by

box counting dimension for the four tested conditions. Mg-Ln, polyLM and Nd1-Ln all have fractal dimensions around 1.7 which is typical of diffusion limited aggregates, whereas pH7-Ln has a distinct, non-fractal dimension of 2. H. Power spectrum for images of all four acellular laminin conditions tested. Note the similarities for Mg-Ln, Nd1-Ln and polyLM despite the differences in synthesis methods.

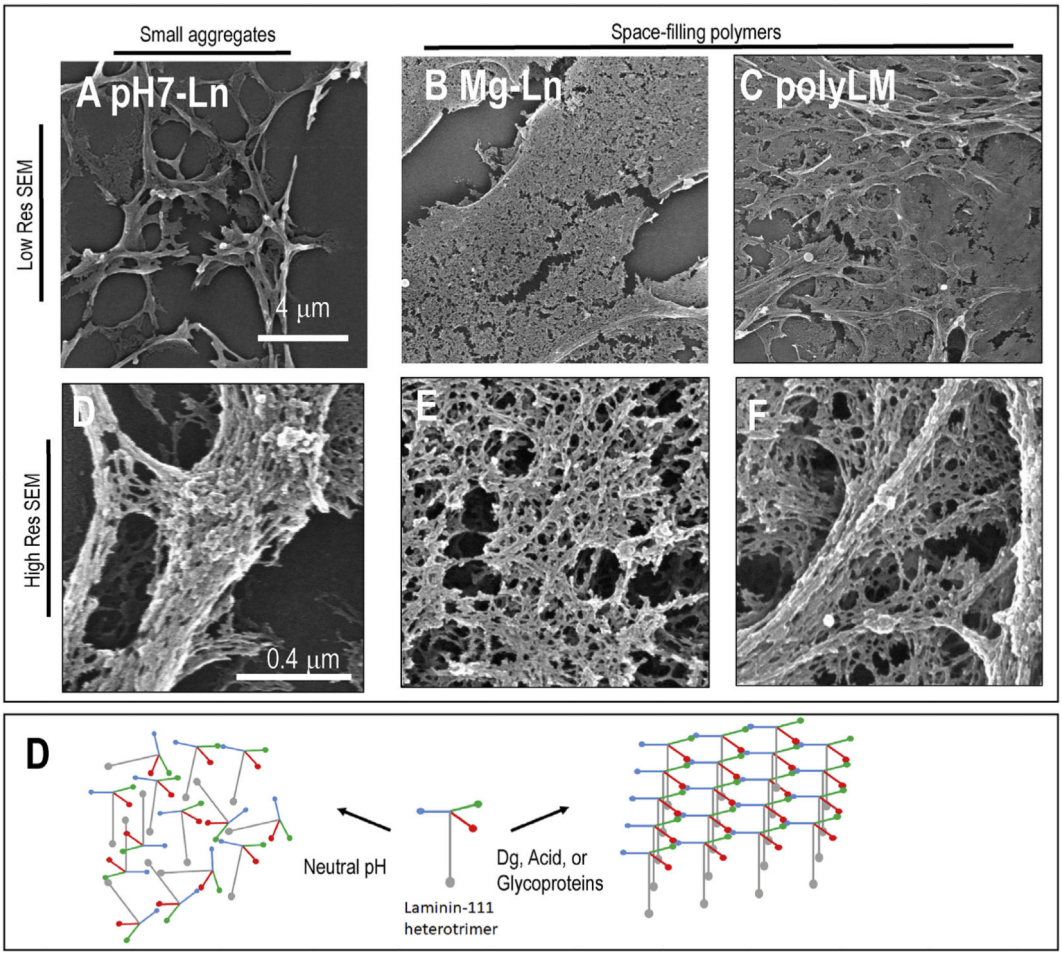

Fig. 2.

Electron microscopy characterization of laminin networks shows similarity between Mg-LN and polyLM at fine scales. A-F. Scanning electron microscopy of pH7-Ln, Mg-Ln and polyLM at 2 resolution scales. Note that at high resolution both Mg-Ln and polyLM share a lacy network structure, whereas pH7-Ln forms globules even at high resolution. G. Cartoon of theorized network structures. In neutral pH laminin assembles randomly, resulting in globules, whereas in the presence of Dg, low pH, or glycoproteins, laminin assembles into networks with a hexagonal lattice at the atomic scale and fractal networks at the ultrastructural scale.

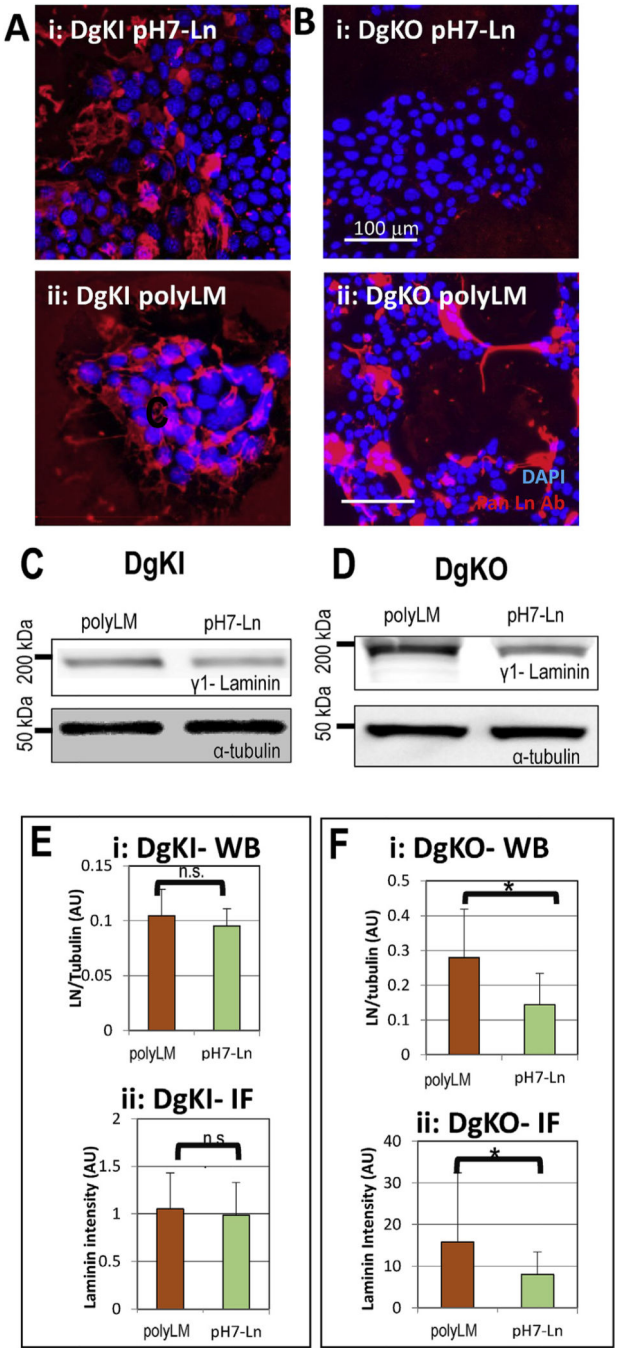

Fig. 3.

Laminin polymerization affects its adherence to DgKO cells. A. Immunofluorescent staining for laminin in DgKI cells treated with pH7-Ln (i) and polyLM (ii) shows similar adhesion of laminin to cells. B. Immunofluorescent staining for laminin in DgKO cells treated with pH7-Ln (i) and polyLM (ii) shows minimal pH7-Ln on the cell surface. C-D. Western blots confirm a difference in laminin adhesion to DgKO treated cells but not to DgKI treated cells, using tubulin as a loading control. E-F. Quantification of western blots (i) and

immunofluorescence (ii) confirms no statistical difference in polyLM and pH7-Ln binding to DgKI, but significantly less pH7-Ln in DgKO cells. (n = 3 experiments).

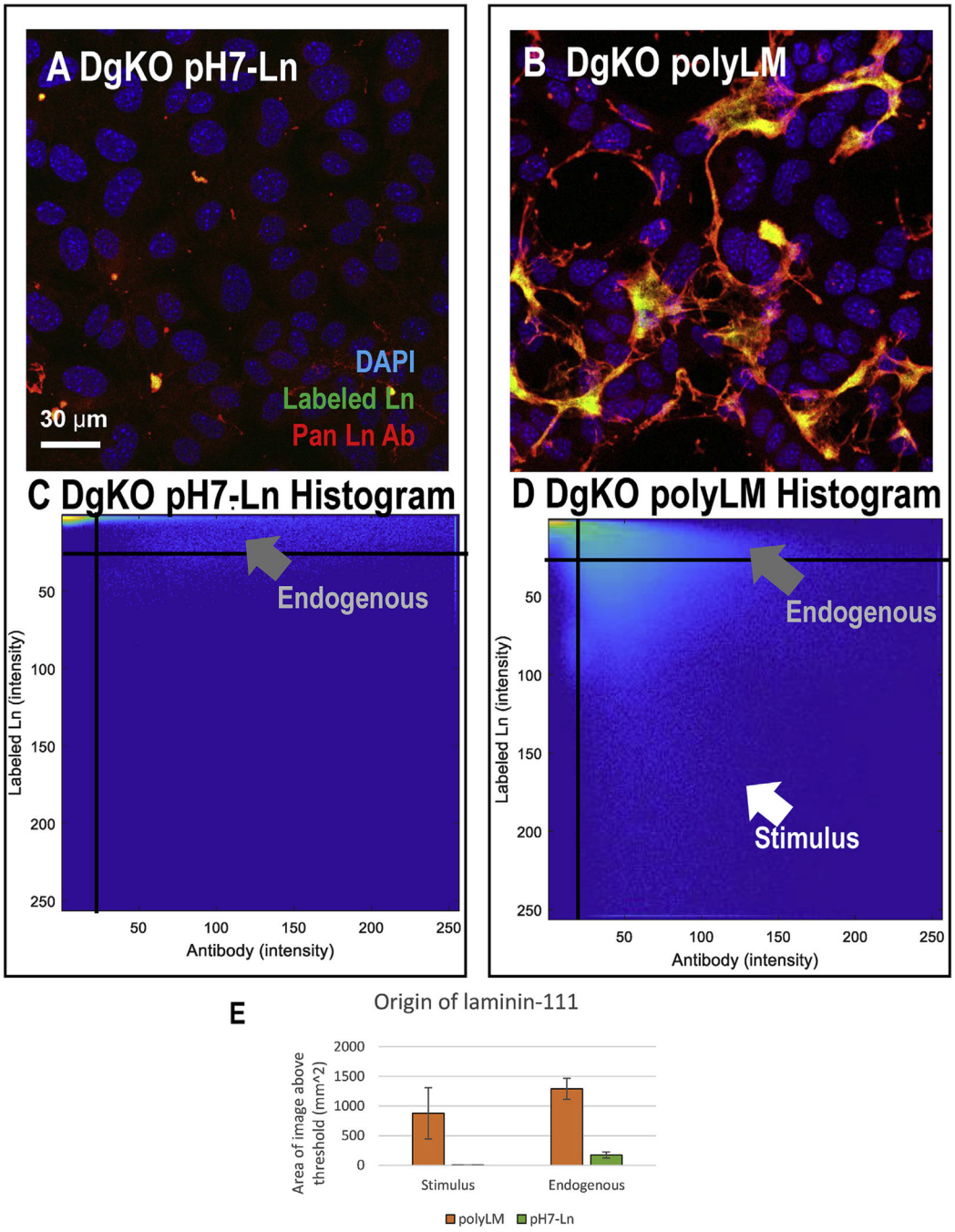

Fig. 4.

Laminin polymerization induces endogenous laminin production. A-B. DgKO cells were treated with fluorescently labeled laminin (A: fluorescent pH7-Ln, B: fluorescent polyLM-in green) then fixed and counterstained using an anti-laminin antibody (in red). C-D. 2D histograms of intensity of the fluorescent tag and antibody staining for these images. In pH7-Ln conditions antibody staining shows low levels of endogenously produced laminins but essentially no labeled exogenous Ln-1 (gray arrow). In polyLM conditions, we observe both exogenous Ln-1 (white arrow-high antibody stain, and high fluorescent label) and formation

of endogenous laminins (gray arrow-high antibody staining, no fluorescent tag). E. Quantification of endogenous and stimulus laminin in pH7-Ln and polyLM conditions.. (For interpretation of the references to colour in this figure legend, the reader is referred to the Web version of this article.)

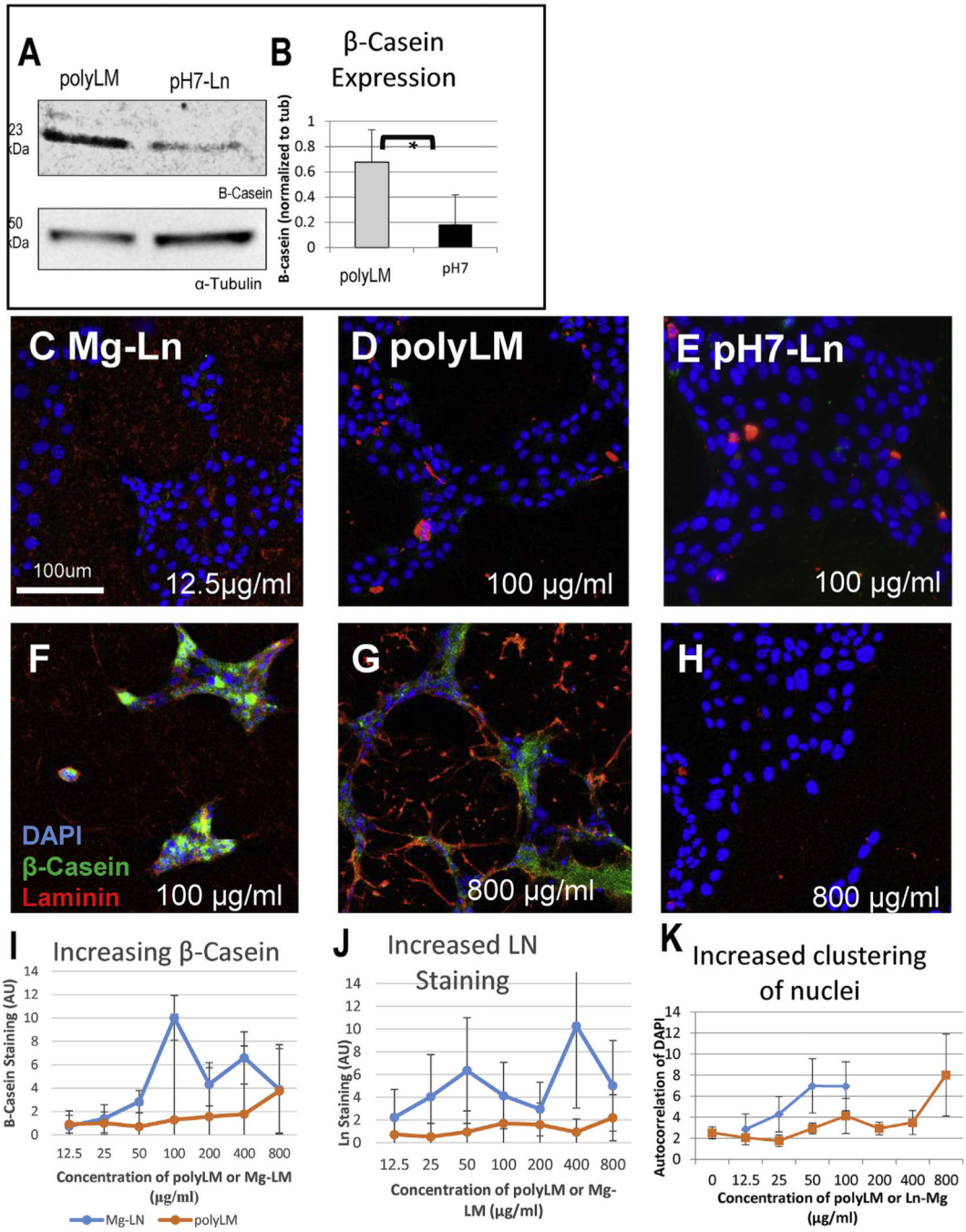

Fig. 5.

Laminin polymerization affects milk protein expression and colony morphology in DgKO cells. A. βcasein expression is higher in polyLM than pH7-Ln stimulated DgKO cells. B. Quantification of western blots shows significantly higher β-casein expression in polyLM conditions (n = 3 experiments). C–H. Cell colony morphology for Mg-Ln at low (C), polyLM at low (D) and pH7-Ln (E) shows flat colonies whereas at high doses both Mg-Ln (E) and polyLM (G) form web like networks with abundant staining for both laminin and β-casein. pH7-Ln at both low and high dose (H–I) shows flat spread colonies with no laminin

binding. I. With increasing doses of either polyLM or Mg-Ln increasing expression of β-casein is observed by immunofluorescent staining and quantitative image processing. β-casein expression in Mg-Ln at 50 μg/ml and polyLM at 800 μg/ml is not statistically different. For pH7-Ln, no dose response behavior was noted; pH7-Ln at 800 μg/ml was not different from pH7-Ln at 12.5 μg/ml. (n =3 experiments). J Ln-1 staining intensity increases with increasing stimulus of either Mg-Ln or polyLM, whereas no change was observed for pH7-Ln (n = 3 experiments). K. Autocorrelation analysis indicates increased clustering of nuclei with increased doses of either Mg-Ln or polyLM. Mg-Ln at 50 or 100 μg/ml and polyLM at 800 μg/ml are statistically different than pH7-Ln at 800 μg/ml. (n =3 experiments).

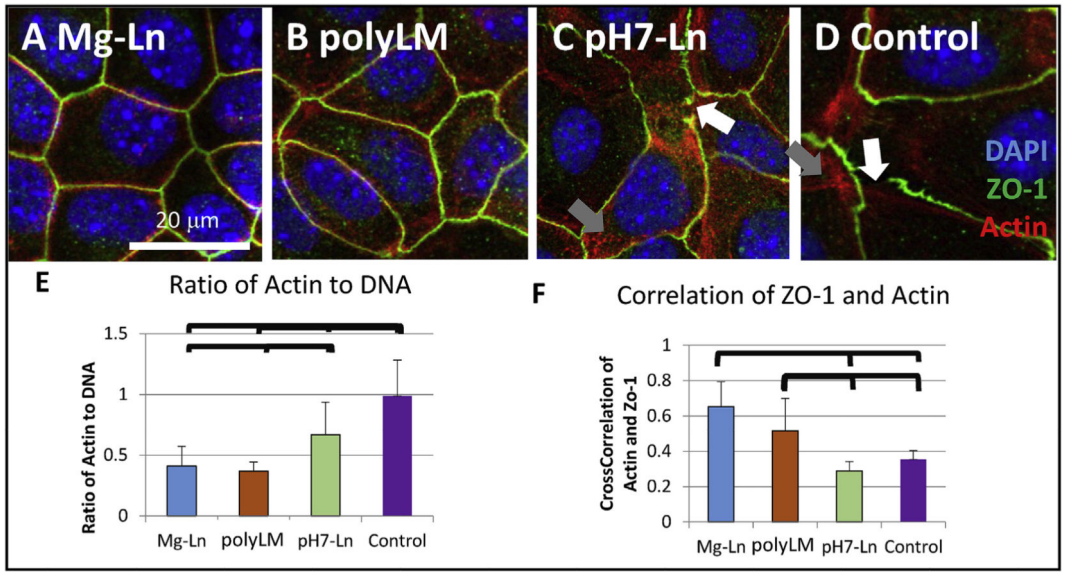

Fig. 6.

Laminin polymerization affects cell morphology in DgKO cells. A-D. Cell-cell junctions vary with laminin treatment. In Mg-Ln conditions (A), apical tight junctions were well-formed and occasional lumens were observed. In polyLM (B), colonies tended to be less well organized, but tight junctions between cells were well organized. In contrast, in pH7-Ln (C) and no-Ln-1 control conditions (D), gaps between cells (white arrows) and abundant actin stress fibers (gray arrows) were observed. E. In Mg-Ln and polyLM conditions, actin and ZO-1 were more likely to be colocalized by cross correlation analysis than in pH7-Ln or control conditions. F. pH7-Ln and control conditions displayed greater actin staining than either Mg-Ln or polyLM conditions as measured by the ratio of the sum of intensity of actin to the sum of intensity of DAPI staining.